

Chapter 16

Introduction to Space-Time Adaptive Processing

16.1 INTRODUCTION

In this chapter, we provide an introduction to Space-Time Adaptive Processing, or STAP. When we discuss radars, we normally consider the processes of beam forming, matched filtering, and Doppler processing separately. By doing this, we are forcing the radar to operate in only one domain at a time: space for beam forming, *fast time* for matched filtering, and *slow time* for Doppler processing. This separation of functions sacrifices capabilities because the radar does not make use of all available information, or *degrees of freedom*.

Suppose we have a linear phased array that has N elements. In terms of beam forming, to maximize the target return and minimize returns from interference (e.g., clutter, jammers, and noise), we say that we have $2N$ degrees of freedom. If we also process K pulses in a Doppler processor, we say we have an additional $2K$ degrees of freedom. With normal processing methods, whereby we separate beam forming and Doppler processing, we have a total of $2K + 2N$ degrees of freedom. If we were to consider that we could simultaneously perform beam forming and Doppler processing, we would have $2KN$ degrees of freedom. This is the premise of the “ST” part of STAP.

Figure 16.1 might provide further help in visualizing this. It contains a depiction of angle-Doppler space. Each of the squares corresponds to a particular angle and Doppler. There are N beam positions and K Doppler cells. The dark square indicates a beam position and Doppler cell that contains interference. With standard processing techniques, we would suppress the interference by independently placing a null at the beam position and Doppler cell containing the interference. The beam null is denoted by the crosshatched squares, and the Doppler null is denoted by the dotted squares. With this approach, the process of suppressing the interference will also cause any signals in the cross-hatched and dotted regions to be suppressed, including target signals. This happens because we separately process in angle and Doppler space.

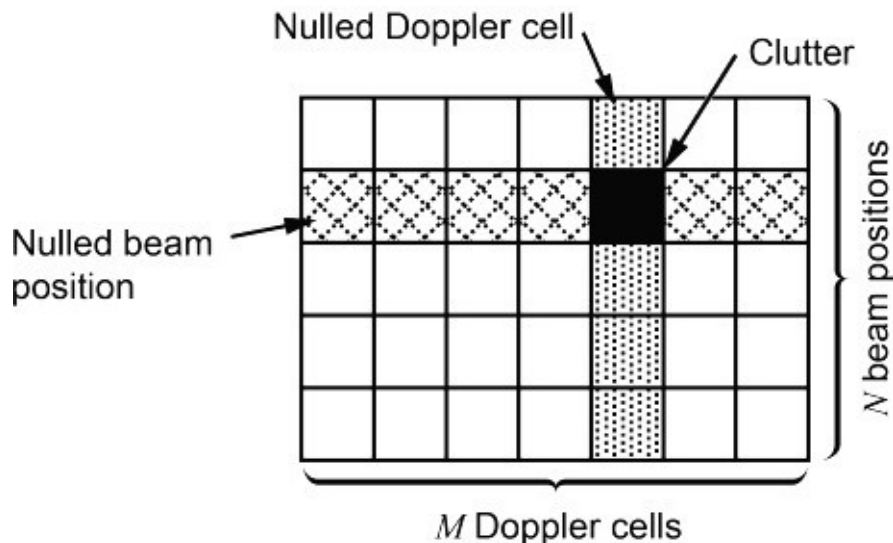


Figure 16.1 Clutter nulling using conventional methods.

With STAP, we would, ideally, simultaneously process in angle and Doppler space. With this simultaneous processing, the processor can be made to place a null at only the angle and Doppler of the interference (at the location of the dark square of Figure 16.1). Thus, it is possible to suppress only interference, and not suppress other signals that might be located at the same angle or Doppler of the interference.

According to [1], it appears that the concept of STAP was first introduced in a 1973 paper by Brennan and Reed [2]. STAP has been, and still is, extensively studied in applications such as SAR, GMTI, MIMO radar, array antennas, tracking radar, SONAR, early warning, and jamming suppression [3–7]. Despite the relatively high processing burden, there are many implemented and fielded STAP platforms [8–10].

We begin the discussion of STAP by first discussing spatial processing (the “S”) and then temporal processing (the “T”). We next discuss how these are combined to perform space-time processing. Following that, we briefly discuss some topics related to the “A,” or adaptive, part of STAP.

The general approach used in STAP is to design the processor to maximize signal-to-interference-plus-noise ratio (SINR) [11–13]. This is the same as the approach used in the matched filter development of Chapter 7. In fact, for the case where the interference is “white” in the space-time domain, the space-time processor is equal to the space-time representation of the signal. That is, the space-time processor is matched to the signal. As a further illustration of the relation between the matched filter and STAP, we note that one of the Cauchy-Schwarz inequalities is used to design the space-time processor [14, 15].

16.2 SPATIAL PROCESSING

As indicated, we begin the STAP development by first considering spatial processing, or *beam forming*. We start by considering the signal and receiver noise and then address a combination of signal, receiver noise and interference, such as jamming or clutter.

16.2.1 Signal Plus Noise

We start with the N element linear array shown in Figure 16.2.¹ In that figure, it is assumed that the target is located at an angle of θ_s relative to broadside. From linear array theory (see Chapter 12) we can write the output of the array as²

$$V(\theta_s) = \sum_{n=0}^{N-1} a_n \sqrt{P_s} e^{-j2\pi n d \sin \theta_s / \lambda} \quad (16.1)$$

where P_s is the signal power from the target at each of the array elements. It is the signal power term of the radar range equation, without the receive directivity term (see Chapter 2).

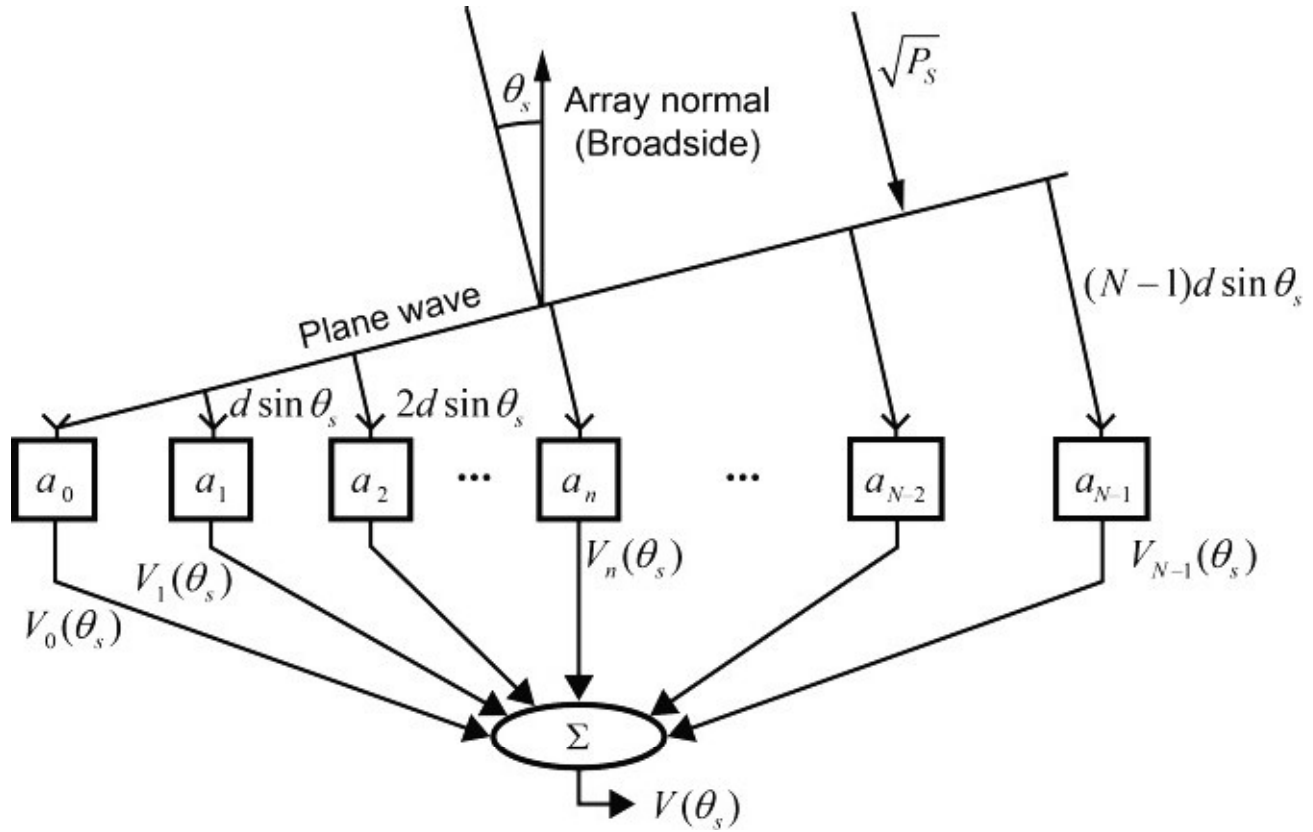


Figure 16.2 Linear phased array.

We define

$$W^H = [a_0 \quad a_1 \quad \cdots \quad a_{N-1}] \quad (16.2)$$

and

$$S(\theta_s) = [s_0 \quad s_1 \quad \cdots \quad s_{N-1}]^T = [1 \quad e^{-j2\pi d \sin \theta_s / \lambda} \quad \cdots \quad e^{-j2\pi(N-1)d \sin \theta_s / \lambda}]^T \quad (16.3)$$

W^H is the weight vector from Chapter 12³ and $S(\theta_s)$ is the target, or signal, *steering vector*. The superscript H denotes the Hermitian, or conjugate-transpose operation [16] (this notation

will come into play shortly). W^H is also sometimes thought of as weights in a spatial filter. Using (16.2) and (16.3), we can write $V(\theta_s)$ as

$$V(\theta_s) = \sqrt{P_s} W^H S(\theta_s) \quad (16.4)$$

We assume there is a separate receiver connected to each element. This makes the noise at each of the antenna elements of Figure 16.2 uncorrelated. This is depicted in Figure 16.3 by the separate n_n in each block. The n_n are complex random variables that we assume are zero-mean and uncorrelated. That is

$$E\{n_n n_l^*\} = 0 \quad n \neq l \quad (16.5)$$

We further stipulate

$$P_N = E\{|n_n|^2\} \quad (16.6)$$

where P_N is the noise power at the input to each of the a_n of Figures 16.2 and 16.3. Equation (16.6) implies the noise power is the same at the output of each receiver. Strictly speaking, this is not necessary. We included it here as a convenience.

The noise voltage at the output of the summer of Figure 16.3 can be written as

$$V_{No} = \sum_{n=0}^{N-1} a_n n_n = W^H \mathbf{N} \quad (16.7)$$

where

$$\mathbf{N} = [n_0 \quad n_1 \quad \cdots \quad n_{N-1}]^T \quad (16.8)$$

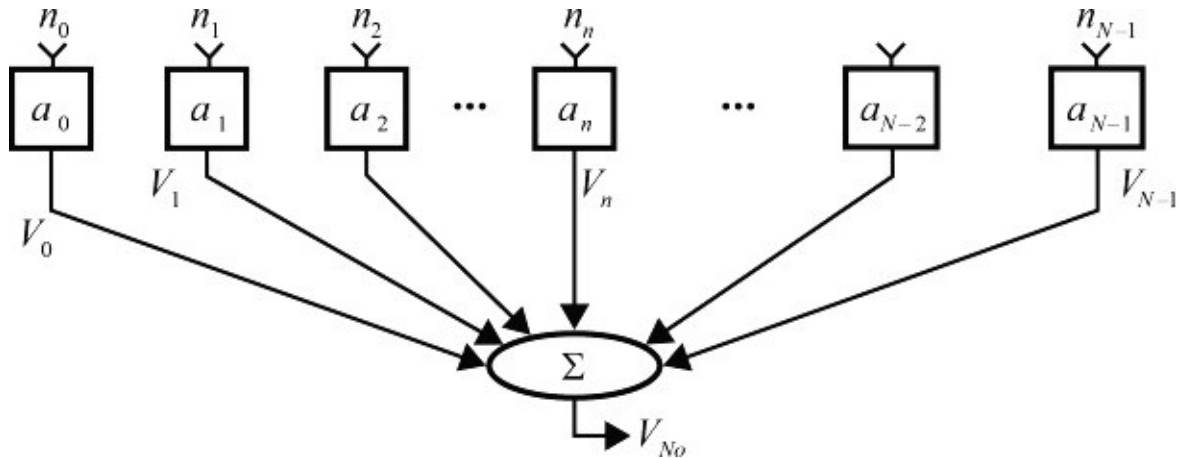


Figure 16.3 Array with only noise.

As a point of clarification, the signal and noise in the above equations are at the output of the matched filter of each receiver. That is, the weights a_n are applied to the signal and noise

at the outputs of the matched filters. More specifically, the signal-plus-noise (plus interference) is sampled at the output of the matched filters and then sent to the processor. Ideally, the samples are taken at a time corresponding to the range delay to the target to be sure that the signal is present in the matched filter output. If the target range delay is not known, several range (time) samples and processors will be needed.

Receivers are needed at each element to implement STAP in its pure form. If we are willing to give up spatial degrees of freedom, receivers could be applied to groups of elements, or *subarrays*. However, with this approach, we limit where the STAP can place nulls. Further discussion of subarraying and STAP can be found in STAP literature [3, 7, 12].

The STAP design criterion is maximization of SINR (SNR for the noise-only case) at the processor output. Therefore we need to develop equations for the signal and noise power at the processor output. From (16.4), the signal power at the processor output is

$$P_{so} = |V(\theta_s)|^2 = P_s |W^H S(\theta_s)|^2 \quad (16.9)$$

Since the noise is a random process, we write the noise power at the output of the summer as

$$P_{no} = E\{|V_{no}|^2\} = E\{|W^H \mathbf{N}|^2\} = W^H E\{\mathbf{N} \mathbf{N}^H\} W = W^H R_N W \quad (16.10)$$

In (16.10)

$$R_N = E\{\mathbf{N} \mathbf{N}^H\} = E\left\{ \begin{bmatrix} n_0 \\ n_1 \\ \vdots \\ n_{N-1} \end{bmatrix} \begin{bmatrix} n_0^* & n_1^* & \cdots & n_{N-1}^* \end{bmatrix} \right\} = P_N I \quad (16.11)$$

and is termed the *receiver noise covariance matrix*. In (16.11), I is the identity matrix. With (16.11), the output noise power becomes

$$P_{no} = P_N W^H W = P_N \|W\|^2 \quad (16.12)$$

The SNR at the output of the summer is

$$SNR = \frac{P_{so}}{P_{no}} = \frac{P_s |W^H S(\theta_s)|^2}{P_N \|W\|^2} \quad (16.13)$$

At this point we invoke one of the Cauchy-Schwarz inequalities [14, 15]. In particular, we use

$$|W^H S(\theta_s)|^2 \leq \|W\|^2 \|S(\theta_s)\|^2 \quad (16.14)$$

with equality when

$$W = \kappa S(\theta_s) \quad (16.15)$$

where κ is an arbitrary, complex constant, which we will set to unity. With this, we get

$$SNR = \frac{P_s |W^H S(\theta_s)|^2}{P_N \|W\|^2} \leq \frac{P_s \|W\|^2 \|S(\theta_s)\|^2}{P_N \|W\|^2} = \frac{P_s \|S(\theta_s)\|^2}{P_N} = \frac{P_s}{P_N} N \quad (16.16)$$

where we made use of

$$\|S(\theta_s)\|^2 = N \quad (16.17)$$

Equation (16.16) tells us that the SNR at the array output has an upper bound equal to the sum of the SNRs at (the outputs of the matched filters of the receivers attached to) each element. Further, the actual SNR at the array output will equal the upper bound if W is chosen according to (16.15), that is W is *matched* to $S(\theta_s)$.

16.2.2 Signal Plus Noise and Interference

We now consider a case where we have interference that is correlated across the array. This interference could be clutter and/or jammers. The appropriate model for this situation is given in Figure 16.4. In this figure, n_{Ii} represents the interference “voltage” and is a zero-mean, complex, random variable. The subscript i is used to represent the i^{th} interference source (which we will need shortly when we consider multiple interference sources). The fact that the same random variable is applied to each of the antenna elements makes the outputs of the elements random variables that are correlated. We write $V_{Ii}(\phi_i)$ as

$$V_{Ii}(\phi_i) = \sum_{n=0}^{N-1} a_n n_{Ii} e^{-j2\pi knd \sin \phi_i / \lambda} = W^H \mathbf{N}_{Ii} \quad (16.18)$$

where

$$\mathbf{N}_{Ii} = n_{Ii} D(\phi_i) \quad (16.19)$$

and

$$D(\phi_i) = \begin{bmatrix} 1 & e^{-j2\pi d \sin \phi_i / \lambda} & \dots & e^{-j2\pi(N-1)d \sin \phi_i / \lambda} \end{bmatrix}^T \quad (16.20)$$

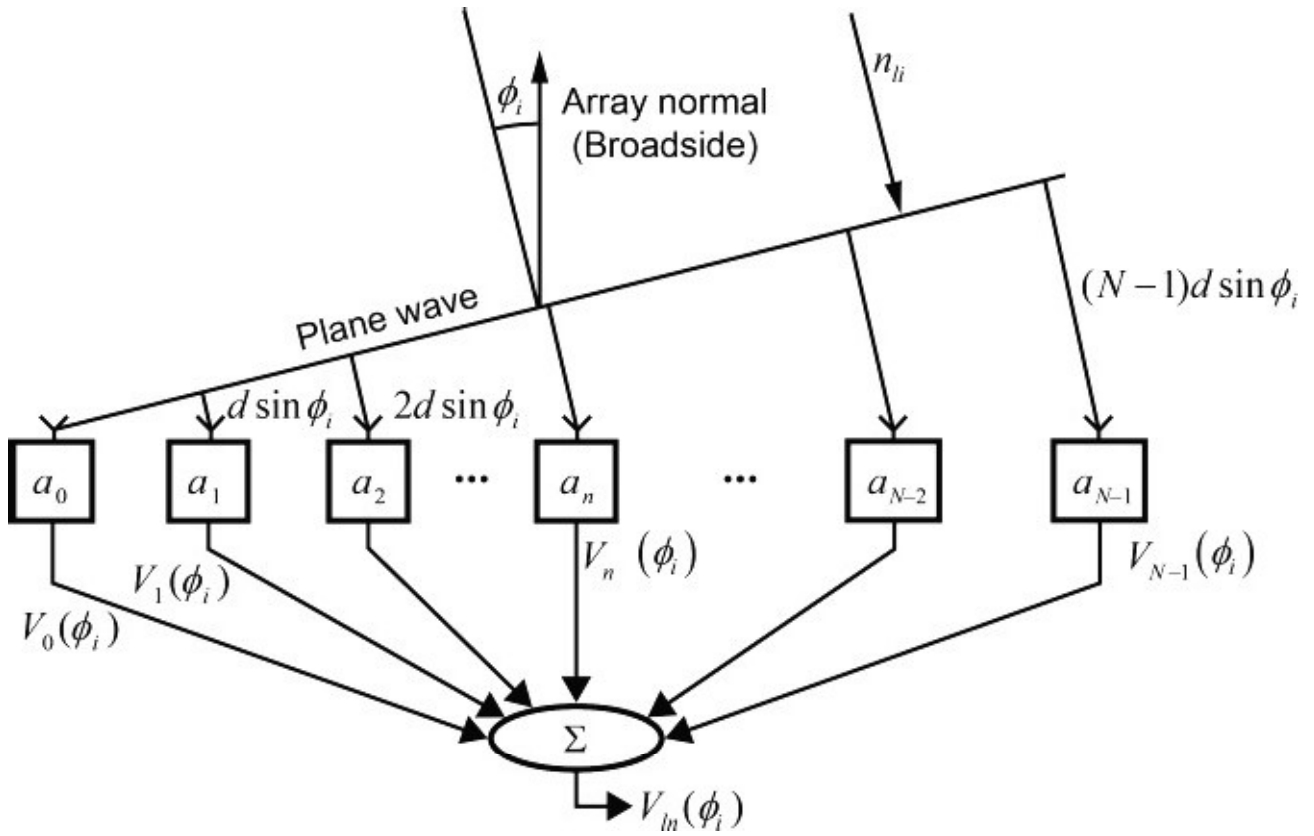


Figure 16.4 Array with interference.

$D(\phi_i)$ is the steering vector for the i^{th} interference source.

We accommodate multiple interference sources by simply summing the voltages for the multiple sources. Specifically,

$$\mathbf{N}_I = \sum_{i=1}^{N_i} \mathbf{N}_{Ii} = \sum_{i=1}^{N_i} n_{li} D(\phi_i) \quad (16.21)$$

We further assume the N_i interference sources are independent so that

$$E\{n_{li} n_{lk}^*\} = \begin{cases} P_{li} & i = k \\ 0 & i \neq k \end{cases} \quad (16.22)$$

The interference power (from the N_i interference sources) is

$$P_{Io} = E\left\{ |W^H \mathbf{N}_I|^2 \right\} = W^H E\{\mathbf{N}_I \mathbf{N}_I^H\} W = W^H R_I W \quad (16.23)$$

In (16.23)

$$\begin{aligned}
R_I &= E\{\mathbf{N}_I \mathbf{N}_I^H\} = \sum_{i=1}^{N_I} \sum_{k=1}^{N_I} E\{n_{Ik} n_{Ik}^*\} D(\phi_i) D^H(\phi_k) \\
&= \sum_{i=1}^{N_I} P_i D(\phi_i) D^H(\phi_i)
\end{aligned} \tag{16.24}$$

where we made use of (16.22).

Combining (16.10) with (16.23), we get the total noise plus interference power as

$$P_{N+I} = P_{No} + P_{Io} = W^H (R_N + R_I) W = W^H R W \tag{16.26}$$

and write the signal-to-interference-plus-noise ratio (SINR) at the output of the summer as

$$\text{SINR} = \frac{P_{So}}{P_{N+I}} = \frac{P_s |W^H S(\theta_s)|^2}{W^H R W} \tag{16.27}$$

As before, we want to choose the spatial filter that maximizes SINR. To do this using the Cauchy-Schwarz inequality, we need to manipulate (16.27). We start by noting that, because of the receiver noise, R will be positive definite [14]. Because of this, we can define a matrix, $R^{1/2}$, such that $R = R^{1/2} R^{1/2}$. Further, $R^{1/2}$ is Hermitian and its inverse, $R^{-1/2}$, exists, and is Hermitian [11, 14]. We use this to write

$$\text{SINR} = \frac{P_s |W^H R^{1/2} R^{-1/2} S(\theta_s)|^2}{W^H R^{1/2} R^{1/2} W} = \frac{P_s |W_R^H S_R(\theta_s)|^2}{\|W_R\|^2} \tag{16.28}$$

where $W_R = R^{1/2} W$ and $S_R(\theta_s) = R^{-1/2} S(\theta_s)$.

Equation (16.28) has the same form as (16.13). Thus, we conclude that the SINR is maximized when

$$W_R = \kappa S_R(\theta_s) \tag{16.29}$$

If we let $\kappa = 1$ and substitute for W_R and $S_R(\theta_s)$ we get the solution

$$W = R^{-1} S(\theta_s) \tag{16.30}$$

The net effect of the above equation is that the weight, W , are, ideally, selected to place the main beam on the target and simultaneously attempt to place nulls at the angular locations of the interference sources. We used the qualifier “ideally” because it is possible that the algorithm will not place the main beam at the target angle or a null at the interference angle. This might happen if the target and interference angles were close to each other (see Exercise 7).

A critical part of this development is that the total interference consists of both receiver noise and other interference sources. The inclusion of receiver noise is what makes the R matrix positive definite and thus nonsingular. If R was singular, R^{-1} would not exist, and we would need to use another approach for finding W . On occasion, R will become ill conditioned because the jammer-to-noise ratio (JNR) is large. If this happens, alternate methods of finding W may be needed. One of these is to use a mean-square criterion such as least-mean-square estimation or pseudo inverse [17–21]. Another is termed *diagonal loading*, which is discussed later.

16.2.3 Example 1

As an example, we consider a 16-element linear array with $\frac{1}{2}$ wavelength element spacing ($d/\lambda = \frac{1}{2}$). We assume that we have a per-element SNR of 0 dB (at the output of the matched filters of the receivers associated with each of the elements). That is, $P_S/P_N = 1$ W/W. We have two noise jammers with per-element JNRs of 40 dB (again, at the outputs of the matched filters). The target is located at an angle of zero, and the jammers are located at angles of $+18^\circ$ and -34° . The selected jammer angles place the jammers on the second and fourth sidelobes of the antenna pattern that results from using uniform illumination (see Figure 16.5). The above specifications lead to the following parameters $P_S = 1$, $P_N = 1$, $P_{I1} = 10^4$, $P_{I2} = 10^4$, $S_S = 0$, $\phi_1 = 18^\circ$, and $\phi_2 = -34^\circ$.

For the first case, we consider only receiver noise (no jammers). From (16.15) with $\kappa = 1$, we have

$$W = S(\theta_s) = S(0) = [1 \quad 1 \quad \cdots \quad 1]^T \quad (16.31)$$

and $\text{SNR}_{\max} = 16P_S/P_S = 16$ W/W or 12.4 dB. The weight vector, W , results in an array with uniform weighting, or uniform illumination (see Chapter 12). A plot of the normalized radiation pattern for this case is shown as the dotted curve in Figure 16.5, which is mostly obscured by the solid curve. As a note, the patterns of Figure 16.5 were generated using

$$R(\theta) = \frac{|V(\theta)|^2}{\max(|V(\theta)|^2)} = \frac{|W^H S(\theta)|^2}{\max(|W^H S(\theta)|^2)} \quad (16.32)$$

where θ was varied from -90° to 90° .⁴

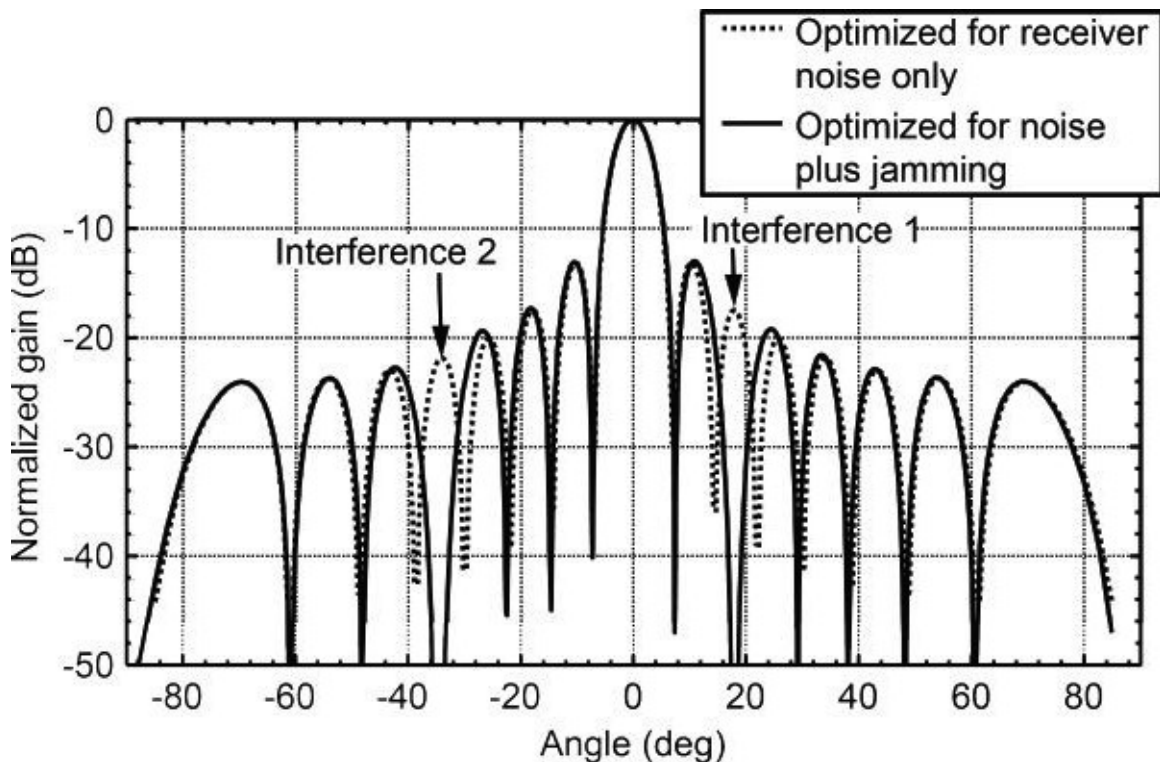


Figure 16.5 Normalized radiation pattern with and without optimization—16-element linear array.

If we use the W given by (16.31) and include the two interference sources, the SINR, at the processor output, is about -24 dB. If we include the interference properties in the calculation of W by using (16.30), the SINR increases to 12 dB, which is close to the noise-only case of about 12.4 dB ($10\log 16$). To accomplish this, the algorithm chose the weights to place nulls in the antenna pattern at the locations of the interference sources. This is illustrated by the solid curve of Figure 16.5, which is a plot of the radiation pattern when the new weights are used.

16.3 TEMPORAL PROCESSING

The temporal processing part of STAP is most often thought of as Doppler processing. In particular, we consider the returns (signal and interference) from several pulses and, similar to spatial processing, weight and sum them. As with spatial processing, we choose the weights to maximize SINR at the output of the processor. The input to the Doppler processor is the output of the matched filter. Thus, we need to characterize the signal, noise, and interference at the matched filter output.

16.3.1 Signal

We consider a transmit waveform that consists of a string of K pulses and write it as

$$v_T(t) = e^{j2\pi f_o t} \sum_{k=0}^{K-1} p(t - kT) \quad (16.33)$$

where $p(t)$ is a general representation of a pulse and T is the spacing between pulses, or pulse repetition interval, PRI (see Chapter 1). As examples, for an unmodulated pulse

$$p(t) = \text{rect}\left[\frac{t}{\tau_p}\right] \quad (16.34)$$

and for an LFM pulse

$$p(t) = e^{j\pi\alpha t^2} \text{rect}\left[\frac{t}{\tau_p}\right] \quad (16.35)$$

where τ_p is the (uncompressed) pulselength and α is the LFM slope (see Chapter 7). The exponential term in (16.33) represents the carrier part of the transmit signal (see Chapter 1).

The normalized return signal, from a point target, is a delayed and scaled version of $v_T(t)$. We define it as

$$v_r(t) = \sqrt{P_s} v_T(t - 2r(t)/c) = \sqrt{P_s} e^{j2\pi f_o(t-2Rr(t)/c)} \sum_{k=0}^{K-1} p(t - 2Rr(t)/c - kT) \quad (16.36)$$

where P_s is the signal power at the matched filter output and $r(t)$ is the range to the target.

If the target is moving at a constant range rate, we can write $r(t)$ as

$$r(t) = r_0 + \dot{r}t \quad (16.37)$$

where r_0 is the target range at $t = 0$ and \dot{r} is the range rate (see Chapter 1). We usually set $t = 0$ at the beginning of the train of K pulses.

With (16.37) $v_r(t)$ becomes

$$v_r(t) = \sqrt{P_s} e^{-j2\pi r_0/\lambda} e^{j2\pi f_o t} e^{j2\pi f_d t} \sum_{k=0}^{K-1} p(t - \tau_r - kT) \quad (16.38)$$

In (16.38), $f_d = -2\dot{r}/\lambda$, $\tau_r = 2r_0/c$ and $\lambda = c/f_o$ is the wavelength of the transmit signal. If we assume that the phase across the pulse is constant, we can write

$$v_r(t) = \sqrt{P_s} e^{-j2\pi r_0/\lambda} e^{j2\pi f_o t} \sum_{k=0}^{K-1} e^{j2\pi f_d kT} p(t - \tau_r - kT) \quad (16.39)$$

In the receiver, we heterodyne to remove the carrier, normalize away the first exponential, and process the signal through the matched filter to obtain

$$v_m(t) = \sqrt{P_s} \sum_{k=0}^{K-1} e^{j2\pi f_d kT} m(t - \tau_r - kT) \quad (16.40)$$

where $m(t)$ is the response of the matched filter to $p(t)$. We assume $m(t)$ is normalized to a peak value of $m(0) = 1$.

For the next step, we sample $v_M(t)$ at times $\tau = \tau_{RC} + kT$. That is, we sample the output of the matched filter once per PRI at a time τ_{RC} relative to the leading edge of each transmit pulse.⁵ The result is a sequence of samples we denote as

$$v_k(f_d) = \sqrt{P_s} e^{j2\pi f_d kT} m_{RC} \quad k \in [0, K-1] \quad (16.41)$$

where m_{RC} is the (generally complex) value of $m(t - \tau_r - kT)$ evaluated at $t = \tau_{RC} + kT$. If we sample the matched filter output at its peak, we will have $\tau_{RC} = \tau_r$ and $m_{RC} = 1$.

16.3.2 Noise

The noise at the matched filter output is also sampled at $t = \tau_{RC} + kT$. This produces a sequence of K , uncorrelated, zero-mean, random variables with equal variances (and mean-square values, or powers) of P_N . We denote these as

$$n_k \quad k \in [0, K-1] \quad (16.42)$$

As a note, it is not necessary that the noise samples be uncorrelated and have equal variances. However, this is the standard assumption when discussing STAP [11].

Assuming we sample the matched filter output at its peak when only signal and noise are present, the signal power in each sample is P_s and the noise power for each sample is P_N . Thus, the SNR at the sampler output, and the input to the processor, is $SNR = P_s/P_N$.

16.3.3 Interference

We assume the interference bandwidth is narrow relative to the transmit waveform PRF (PRF = $1/T$). More specifically, we assume the interference signal at the sampler output is a wide-sense stationary, zero-mean random process with an autocorrelation given by

$$R_I(k) = E\{v_I(k+l)v_I^*(l)\} \quad (16.43)$$

where $v_I(k)$ is the interference voltage at the sampler output. It is equal to the output of the matched filter, sampled at $t = \tau_{RC} + kT$, when the input is the signal returned from the interference.

In general, $R_I(k)$ is a complicated function of k . For the special case where the interference is a tone with a Doppler frequency of f_I and a random amplitude with a mean-square value (power) of P_I , $R_I(k)$, becomes

$$R_I(k) = P_I e^{j2\pi f_I kT} \quad k \in [0 \quad K-1] \quad (16.44)$$

16.3.4 Doppler Processor

We assume the Doppler processor is a K -length finite impulse response (FIR) filter with coefficients of ω_k . If the input to the processor is $v_{in}(k)$, the output, after K samples have been processed, is

$$V_{Io} = \sum_{k=0}^{K-1} \omega_k v_{in}(k) = \Omega^H V_{in} \quad (16.45)$$

where

$$\Omega^H = [\omega_0 \quad \omega_1 \quad \cdots \quad \omega_{K-1}] \quad (16.46)$$

and

$$V_{in} = [v_{in}(0) \quad v_{in}(1) \quad \cdots \quad v_{in}(K-1)]^T \quad (16.47)$$

When the input is the signal, we have, from (16.41)

$$v_{in}(k) = v_k(f_d) = \sqrt{P_S} e^{j2\pi f_d kT} m_{RC} \quad (16.48)$$

If we further assume the sampler samples the matched filter output at $t = \tau_R + kT$, we have $m_{RC} = 1$. Using (16.47) we have

$$V_{in}^{signal} = \sqrt{P_S} S(f_d) = \sqrt{P_S} [1 \quad e^{j2\pi f_d T} \quad \cdots \quad e^{j2\pi f_d (K-1)T}]^T \quad (16.49)$$

The signal voltage at the Doppler processor output is

$$V_{So}(f_d) = \sqrt{P_S} \Omega^H S(f_d) \quad (16.50)$$

For the noise, we write

$$V_{in}^{noise} = \mathbf{N} = [n_0 \quad n_1 \quad \cdots \quad n_{K-1}]^T \quad (16.51)$$

and the output of the Doppler processor is

$$V_{No} = \Omega^H \mathbf{N} \quad (16.52)$$

We write the interference input to the Doppler processor as

$$V_{in}^{interference} = \mathbf{N}_I = [v_I(0) \ v_I(1) \ \cdots \ v_I(K-1)]^T \quad (16.53)$$

and the processor output as

$$V_{Io} = \Omega^H \mathbf{N}_I \quad (16.54)$$

As with the spatial processing case, we choose the Ω that maximizes SINR at the Doppler processor output. Thus, we need an equation for the peak signal power, P_{So} , and the total, average interference power, $P_{No} + P_{Io}$, at the processor output. By using the sum of the noise and interference powers, we are assuming the receiver noise and the interference are uncorrelated. This is a standard assumption.

The peak signal power is

$$P_{So} = |V_{So}(f_d)|^2 = P_S |\Omega^H S(f_d)|^2 \quad (16.55)$$

and the average noise power is

$$P_{No} = E\{|V_{No}|^2\} = \Omega^H E\{\mathbf{N}\mathbf{N}^H\} \Omega \quad (16.56)$$

Since we assumed the noise samples were uncorrelated and had equal power,

$$E\{\mathbf{N}\mathbf{N}^H\} = P_N I \quad (16.57)$$

and

$$P_{No} = P_N \|\Omega\|^2 \quad (16.58)$$

The interference power at the processor output is

$$P_{Io} = E\{|V_{Io}|^2\} = \Omega^H E\{\mathbf{N}_I \mathbf{N}_I^H\} \Omega = \Omega^H R_I \Omega \quad (16.59)$$

where

$$\begin{aligned}
R_I &= E\{\mathbf{N}_I \mathbf{N}_I^H\} = E\left\{\begin{bmatrix} v_I(0) \\ v_I(1) \\ \vdots \\ v_I(K-1) \end{bmatrix} \begin{bmatrix} v_I^*(0) & v_I^*(1) & \cdots & v_I^*(K-1) \end{bmatrix}\right\} \\
&= \begin{bmatrix} R_I(0) & R_I(-1) & \cdots & R_I(1-K) \\ R_I(1) & R_I(0) & \cdots & R_I(0) \\ \vdots & \vdots & \ddots & \vdots \\ R_I(K-1) & R_I(K-2) & \cdots & R_I(0) \end{bmatrix}
\end{aligned} \tag{16.60}$$

where $R_I(k)$ is defined in (16.43).

For the case where the interference is a tone,

$$R_I = E\{\mathbf{N}_I \mathbf{N}_I^H\} = P_I D(f_I) D^H(f_I) \tag{16.61}$$

where

$$D(f_I) = \begin{bmatrix} 1 & e^{j2\pi f_I T} & \cdots & e^{j2\pi f_I (K-1)T} \end{bmatrix}^T \tag{16.62}$$

For multiple interference sources

$$R_{IT} = \sum_i R_{Ii} \tag{16.63}$$

where the sum is taken over the total number of interference sources.

The SINR at the Doppler processor output is

$$SINR = \frac{P_{So}}{P_{No} + P_{Io}} = \frac{P_S |\Omega^H S(f_d)|^2}{\Omega^H R \Omega} = \frac{P_S |\Omega^H S(f_d)|^2}{\Omega^H (R_{IT} + P_N I) \Omega} \tag{16.64}$$

This is the same form as in the spatial processing case. Applying those results here gives

$$\Omega = R^{-1} S(f_d) \tag{16.65}$$

16.3.5 Example 2

As an example, we consider a Doppler processor with $K = 16$. We assume an input SNR of 0 dB (at the output of the matched filter). That is, $P_S/P_N = 1\text{W/W}$. We also assume we sample the matched filter output at $t = \tau_R + kT$. We have two tone interferences with JNRs of 40 dB (again,

at the output of the matched filter). We assume a PRF of 1,000 Hz, which gives $T = 0.001$ s. The target is located at a Doppler frequency of zero, and the interferences are located at Doppler frequencies of 217 Hz and -280 Hz. These Doppler frequencies place the interferences on the second and fourth sidelobes of the Doppler processor frequency response that results from using uniform weighting. The above specifications lead to the following parameters: $P_S = 1$, $P_N = 1$, $P_{I1} = 10^4$, $P_{I2} = 10^4$, $f_d = 0$, $f_{I1} = 217$ Hz, and $f_{I2} = -280$ Hz.

For the first case, we consider only receiver noise. From (16.65) with $R = P_N I$ we have

$$\Omega = S(f_d) = S(0) = [1 \ 1 \ \dots \ 1]^T \quad (16.66)$$

And $SNR_{max} = 16 P_S/P_N = 16$ W/W or 12.4 dB. The weight vector, Ω results in a Doppler processor with uniform weighting. A plot of the normalized frequency response of the Doppler processor is shown as the dotted curve in Figure 16.6, which is mostly obscured by the solid curve. As a note, the frequency responses of Figure 16.6 were generated using

$$F(f) = \frac{|\Omega^H S(f)|^2}{\max(|\Omega^H S(f)|^2)} \quad (16.67)$$

where f was varied from $-PRF/2$ to $PRF/2$, or -500 Hz to 500 Hz.

If we use the Ω given by (16.66) and include the two interferences, the SINR, at the processor output, is about -22 dB. If we include the interference in the calculation of Ω by using (16.65), the SINR increases to 12 dB, which is close to the noise-only case of about 12.4 dB ($10\log 16$). To accomplish this, the algorithm chose the weights to place nulls in the frequency response of the Doppler processor at the Doppler frequencies of the interferences. This is illustrated by the solid curve of Figure 16.6, which is a plot of the frequency response when the new weights are used.

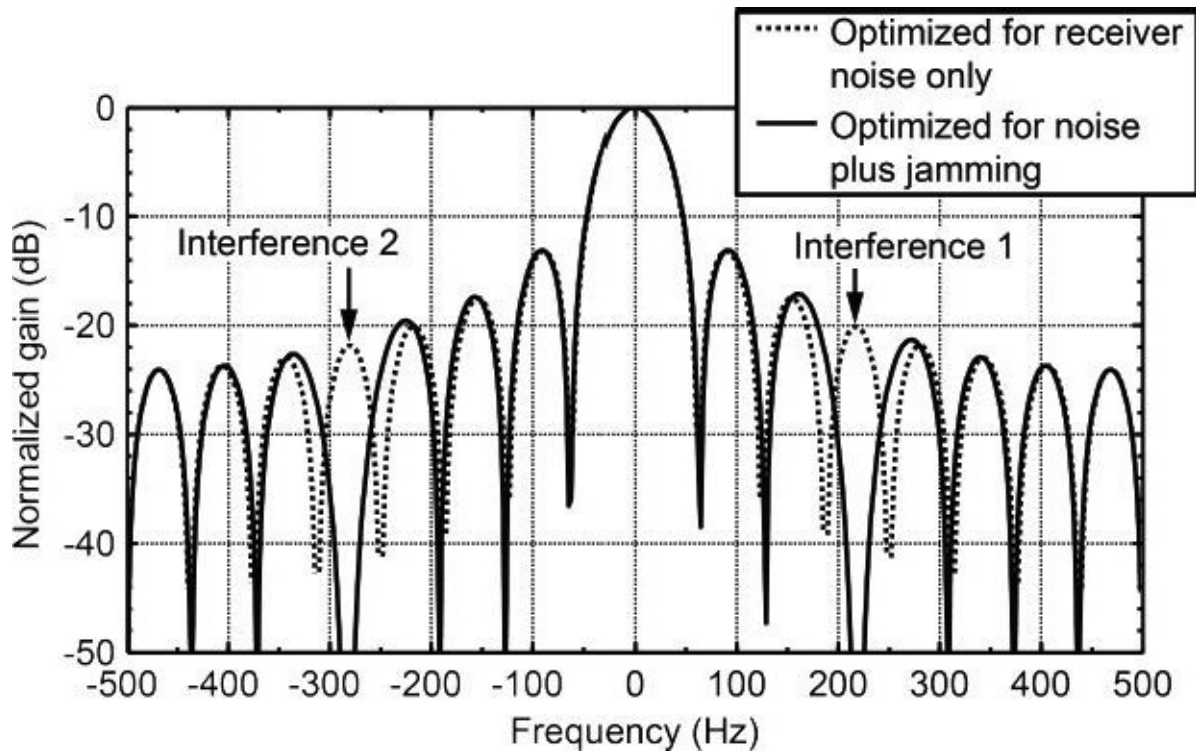


Figure 16.6 Normalized frequency response with and without optimization—16 tap Doppler processor.

16.4 ADAPTIVITY ISSUES

We have discussed both the space and time parts of STAP. However, we have not addressed the adaptive part. Since the target and interference angles and Dopplers could change every dwell (sequence of K pulses), the target steering vector and the R matrices must be recomputed on each dwell. This means that new weights would be computed on each dwell to *adapt* to the target and interference environment—thus the adaptive part. In Section 16.6, we discuss another aspect of adaptivity that involves measuring the environment to estimate the R matrix.

16.5 SPACE-TIME PROCESSING

We now address the issue of combined space and time processing. In space-time processing, rather than form a function of angle or a function of Doppler, we combine spatial and temporal equations for the signal [(16.1) and (16.50)] to form a combined function of angle and Doppler at the output of the space-time processor. In equation form, we write

$$\begin{aligned}
 V(\theta_s, f_d) &= \sqrt{P_s} \left(\sum_{n=0}^{N-1} a_n e^{-j2\pi n d \sin \theta_s / \lambda} \right) \left(\sum_{k=0}^{K-1} \omega_k e^{j2\pi k f_d T} \right) \\
 &= \sqrt{P_s} \sum_{k=0}^{K-1} \sum_{n=0}^{N-1} a_n \omega_k e^{-j2\pi n d \sin \theta_s / \lambda} e^{j2\pi k f_d T}
 \end{aligned} \tag{16.68}$$

We recognize the above as a sum of KN terms. Generalizing the product of the weights to KN distinct weights we get

$$V(\theta_s, f_d) = \sqrt{P_s} \sum_{n=0}^{N-1} \sum_{k=0}^{K-1} w_{n,k} e^{-j2\pi n d \sin \theta_s / \lambda} e^{j2\pi k f_d T} \quad (16.69)$$

We next organize the weights into a general weight vector, \mathbf{w} , and the $e^{-j2\pi n d \sin \theta_s / \lambda}$ $e^{j2k f_d T}$ terms into a generalized steering vector, S , and write $V(\theta_s, f_d)$ in matrix form as

$$V(\theta_s, f_d) = \sqrt{P_s} \mathbf{w}^H S(\theta_s, f_d) \quad (16.70)$$

Extending the interference representation of Sections 16.2 and 16.3, we can write the interference at the space-time processor output as

$$V_{N+I} = \mathbf{w}^H \mathbf{N}_{N+I} \quad (16.71)$$

where

$$\mathbf{N}_{N+I} = \mathbf{N} + \mathbf{N}_I = \mathbf{N} + \sum_{i=1}^{N_I} n_i D(\phi_i, f_i) \quad (16.72)$$

In (16.72), \mathbf{N} is the receiver noise and $D(\phi_i, f_i)$ is the steering vector to the interference in angle-Doppler space. With this representation of interference, we are limiting ourselves to tone interferences.

We use the techniques discussed in Sections 16.2 and 16.3 to place the “main beam” in angle-Doppler space on the target and to place nulls at the angle-Doppler locations of the interferences. Specifically, we find that the optimum weight vector is given by

$$\mathbf{w} = \kappa R^{-1} S(\theta_s, f_d) \quad (16.73)$$

where

$$R = E \left\{ \mathbf{N}_{N+I} \mathbf{N}_{N+I}^H \right\} \quad (16.74)$$

and K is an arbitrary, complex constant that we normally set to unity.

At this point, we need to further discuss the signal and interference steering vectors, $S(\theta_s, f_d)$ and $D(\theta_r, f_r)$, and how to compute R . We note that the exponential terms of (16.68) and (16.69) contain all possible KN combinations of $e^{-j2\pi n d \sin \theta_s / \lambda}$ and $e^{j2k f_d T}$. We organize the N exponentials containing θ_s into a vector

$$S(\theta_s) = \begin{bmatrix} 1 & e^{-j2\pi d \sin \theta_s / \lambda} & \dots & e^{-j2\pi (N-1) d \sin \theta_s / \lambda} \end{bmatrix}^T \quad (16.75)$$

and the K exponentials containing f_d in to a vector

$$S(f_d) = \begin{bmatrix} 1 & e^{j2\pi f_d T} & \dots & e^{j2\pi(K-1)f_d T} \end{bmatrix}^T \quad (16.76)$$

We next use these vectors to form a matrix

$$\mathbf{S}(\theta_s, f_d) = S(\theta_s) S^T(f_d) \quad (16.77)$$

that contains all KN combinations of the elements of $S(\theta_s)$ and $S(f_d)$. To form the KN element vector, $S(\theta_s, f_d)$, we concatenate the columns of $\mathbf{S}(\theta_s, f_d)$. The $D(\theta_r, f_r)$ vector for each interference source is formed in a similar fashion.

From (16.72) and (16.74), we can form R as

$$\begin{aligned} R &= E\{\mathbf{N}_{N+I}\mathbf{N}_{N+I}^H\} = E\{(\mathbf{N} + \mathbf{N}_I)(\mathbf{N} + \mathbf{N}_I)^H\} \\ &= E\{\mathbf{N}\mathbf{N}^H\} + E\{\mathbf{N}_I\mathbf{N}_I^H\} = R_N + R_I \end{aligned} \quad (16.78)$$

where we made use of the standard assumption that the receiver noise, \mathbf{N} , and interference, \mathbf{n}_I , are independent.

There are N receivers and matched filters, and each receiver processes K pulses through the matched filter and sampler. Thus, we will have KN receiver noise samples. We assume they are all zero-mean, uncorrelated, and have equal powers of P_N . Thus,

$$R_N = P_N I \quad (16.79)$$

where I is an KN by KN identity matrix.

For each interference we have

$$\begin{aligned} R_{Ii} &= E\left\{\left[n_{Ii}D(\phi_i, f_i)\right]\left[n_{Ii}D(\phi_i, f_i)\right]^H\right\} = E\{|n_{Ii}|^2\}D(\phi_i, f_i)D^H(\phi_i, f_i) \\ &= P_{Ii}D(\phi_i, f_i)D^H(\phi_i, f_i) \end{aligned} \quad (16.80)$$

where P_{Ii} is the power associated with the i^{th} interference. With this we get

$$R = P_N I + \sum_i P_{Ii}D(\phi_i, f_i)D^H(\phi_i, f_i) \quad (16.81)$$

where the sum is taken over the total number of interference sources.

With some thought, it should be clear that the dimensionality of the STAP problem has increased substantially, when compared to only spatial or temporal processing. If we perform STAP separately in angle and Doppler, we would need to compute $K + N$ weights. If we simultaneously perform STAP in angle and Doppler space, we must compute KN weights. To complicate the problem further, remember that we need to compute a separate set of weights

for each range cell that is processed. This represents a considerable computational burden. To minimize the burden, much of today's research in STAP is concerned with avoiding the computation of KN weights, while still trying to maintain acceptable performance [11].

16.5.1 Example 3

As an illustration of the space-time processing, we extend Examples 1 and 2 to a full space-time processor. We again assume a 16-element array and a Doppler processor that uses 16 pulses. We use the classical STAP approach and process all $16 \times 16 = 256$ signal-plus-noise-plus-interference samples in one processor with 256 weights. (Recall that we do this for each range cell of interest.) We assume the target is located at an angle of zero and a Doppler frequency of zero. The element spacing is $\frac{1}{2}$ wavelength and the PRF is 1,000 Hz. The single-pulse, per-element SNR is 0 dB (at the outputs of the matched filters). We consider two tone interference sources. They are located at angles of $+18^\circ$ and -34° . Their Doppler locations, corresponding to the above angles, are 217 Hz and -280 Hz respectively. The JNRs of the two interference sources are 50 dB. With these specifications, we get the following parameters: $P_S = 1$, $\theta_s = 0$, $f_d = 0$, $P_N = 1$, $P_{I1} = 10^5$, $P_{I2} = 10^5$, $\phi_1 = 18^\circ$, $\phi_2 = -34^\circ$, $f_1 = 217$ Hz and $f_2 = -280$ Hz.

We compute R using (16.79) through (16.81). Since $\theta_S = 0$ and $f_d = 0$

$$S(\theta_s, f_d) = S(0, 0) = [1 \quad 1 \quad \cdots \quad 1]^T \quad (16.82)$$

or a vector of 256 ones. Finally, we compute w using (16.73) with $k = 1$.

In an actual STAP implementation, we would compute the output of the STAP processor using

$$V_o = w^H V_{in} \quad (16.83)$$

where V_{in} is a vector that contains the KN outputs from the samplers in each receiver. The first N elements of V_{in} are the outputs from the N receivers on the first pulse. The next N elements are the outputs from the N receivers on the second pulse, and so forth.

For this example problem, we want to generate a three-dimensional plot of the processor output as a function of angle and frequency. We can do this in several ways. One would be to use (16.70) and compute

$$G(\theta, f) = \frac{|w^H S(\theta, f)|^2}{\max(|w^H S(\theta, f)|^2)} \quad (16.84)$$

for θ and f of interest. An alternate method would be to use the FFT to implement [see (16.69)]

$$V(\theta, f) = \sum_{n=0}^{N-1} \sum_{k=0}^{K-1} w_{n,k} e^{-j2\pi nd \sin \theta / \lambda} e^{j2\pi kfT} \quad (16.85)$$

and use

$$G(\theta, f) = \frac{|V(\theta, f)|^2}{\max(|V(\theta, f)|^2)} \quad (16.86)$$

This was the method used to generate the plots of Figures 16.7 and 16.8. The weight vector is formed into a two-dimensional weight matrix, \mathbf{W} , by reversing the algorithm used to form $S(\theta_s, f_d)$ and $D(\phi_r, f_r)$. That is, we let the first column of \mathbf{W} be the first N elements of \mathbf{w} , the second column be the second N elements, and so forth. We next compute $V(\theta, f)$ by computing the Fourier transform of \mathbf{W} using a two-dimensional (2-D) FFT. Finally, $G(\theta, f)$ is computed using (16.86).

The results of this process are shown in Figures 16.7 and 16.8. The figures are contour plots where shading is used to indicate power in dB. The bar to the right provides the relation between power level and shading. The y-axis is $\sin(\theta)$ and has the units of sines (see Chapter 12). This vertical axis scaling was chosen because it was compatible with the routine used to generate the plots. A 512 by 512, 2-D FFT (rather than a 16 by 16, 2-D FFT) was used to generate the plots. This was done to provide a plot that showed the gradations in power level.

Figure 16.7 is a plot of $G(\theta, f)$ for the case where the interference consisted of only receiver noise. Since the target was located at $(\theta_s, f_d) = (0,0)$, the resulting weight, \mathbf{w} , was a vector of 256 ones. As expected, the peak of $G(\theta, f)$ occurs at $(0,0)$. Note that the two interference sources are located on the peaks of two angle-Doppler sidelobes $G(\theta, f)$. Because of this, the only rejection of these sources offered by the processor is due to the amplitudes of the sidelobes relative to the response at $(0,0)$. The SINR for this case was -13.4 dB. When the interference sources were omitted, the SNR was the expected, noise-limited value of $10\log(256) = 24.1$ dB.

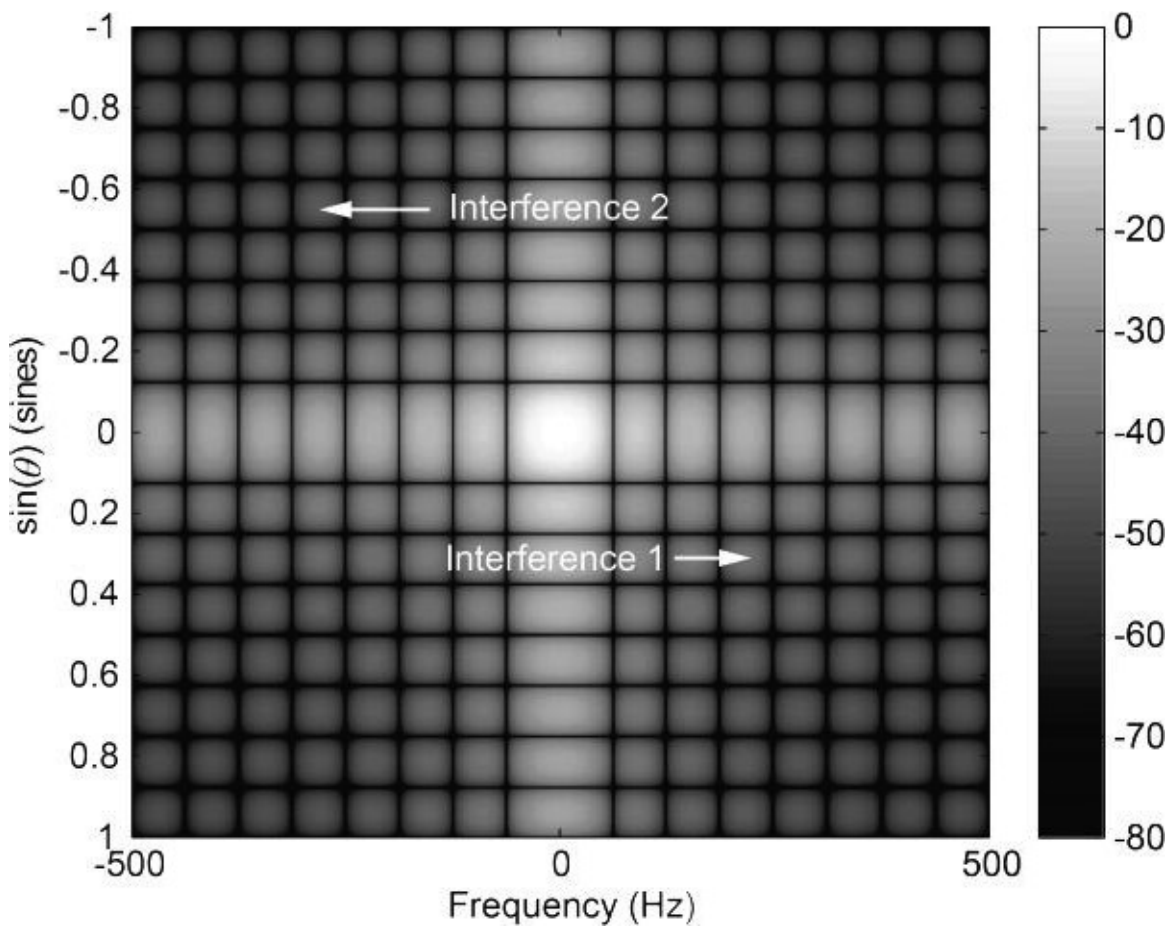


Figure 16.7 Angle-Doppler map—weights based on only receiver noise.

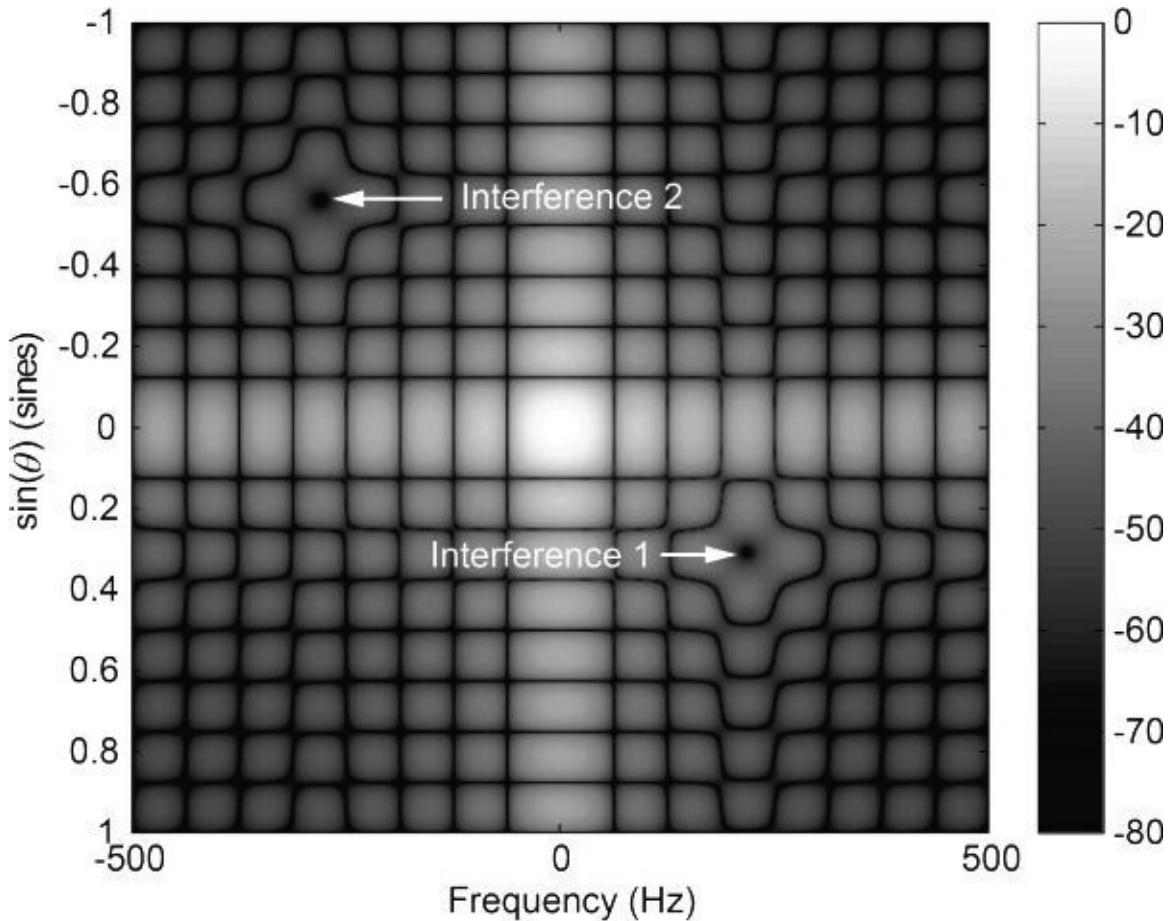


Figure 16.8 Angle-Doppler map—two interference sources included in weight computation.

Figure 16.8 is a plot of $G(\theta,f)$ for the case where the interference sources were included in the weight computation. The two nulls at the locations of the interferences are clearly visible, as is the main beam at $(0,0)$. With this set of weights, the SINR was 24.1 dB, which is the noise-limited value.

As an experiment, the optimization was extended to include two desired targets: one at $(0,0)$ and another at $(\theta_{s2},f_{d2}) = (39^\circ, 217 \text{ Hz})$. Both targets had the same normalized power of $P_{S1} = P_{S2} = 1$. The second target was also placed so that its Doppler frequency was the same as one of the interference sources. However, it was separated in angle from the interference source. The other interference source was left at location shown in Figures 16.7 and 16.8.

Figure 16.9 contains $G(\theta,f)$ for the case where the weight computation was based on only receiver noise. As can be seen, the calculated weights are such that there are two main lobes at the locations of the two targets. The distortion in the angle-Doppler map is due to the interaction of the two targets. Specifically, the targets were placed so that one was on the peak of a sidelobe of the other. When the interference sources were omitted, the SNR was about 21.1 dB for each of the targets. However, when the interference sources were included, the SINR for each of the targets was -31.1 . The noise-only SNR of 21.1 is 3 dB less than the single target case because of the presence of two targets rather than one.

Figure 16.10 corresponds to the case where the two interference sources were included in the computation of \mathbf{w} . As would be expected, the peaks at the locations of the targets are still present. However, the weights have altered the angle-Doppler sidelobe structure to place a null at the angle location of the interference sources that was at the same Doppler frequency as one of the targets. For this case, the combined SINR at the output of the processor was about 21.2 dB for target 1 [the target at $(0,0)$] and 21 dB for the other target, which is about the same as the noise only case. This indicates that the weight calculation algorithm chose the weights so that both interference sources were greatly attenuated.

We note that the examples of this section are “academic.” In practice, it is unlikely that interference would be at only two specific angle-Doppler locations (or that we would want to place beams on two targets at the same time). More likely, the interference would be a line through angle-Doppler space. This might be the situation encountered in an airborne radar application where STAP was used to mitigate ground clutter. We consider this in the next example.

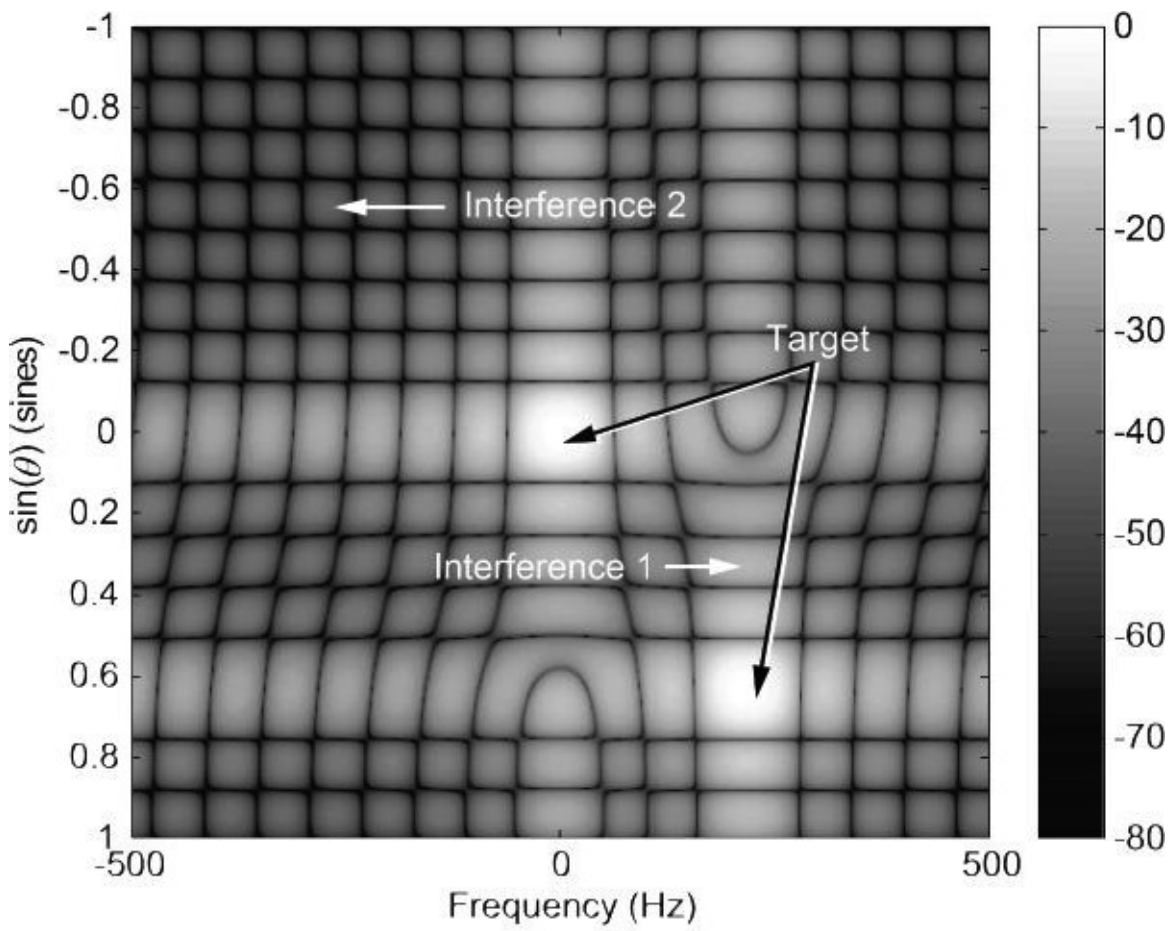


Figure 16.9 Angle-Doppler map—weights based on only receiver noise—two targets.

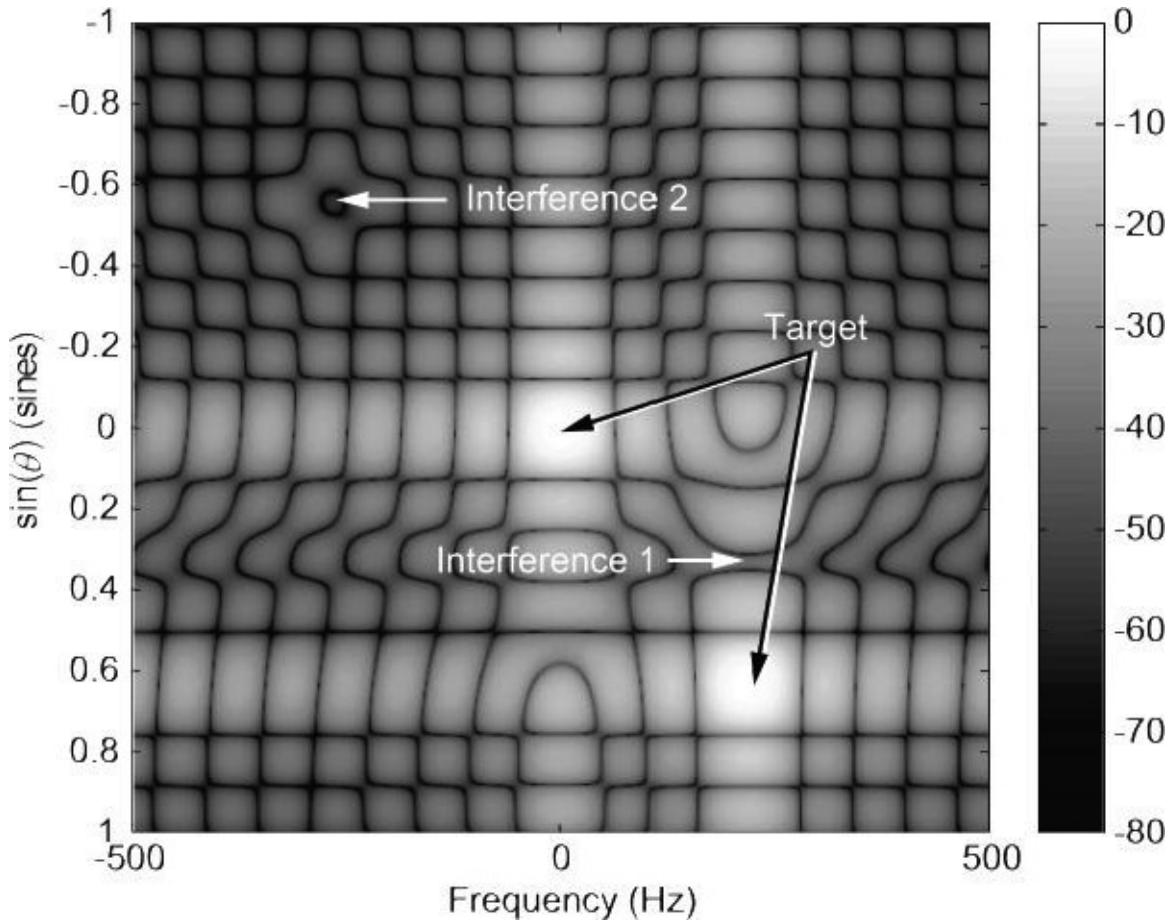


Figure 16.10 Angle-Doppler map—two interference sources included in weight computation—two targets.

16.5.2 Example 4

As another example of STAP, we consider the simplified airborne radar problem shown in Figure 16.11. The aircraft in the center of the concentric circles contains a search radar (e.g., AWACS—airborne warning and control system) that is flying at an altitude of 3 km, in the direction of the arrow, at a velocity of 100 m/s. The target is also at an altitude of 3 km and is flying in the direction shown at a velocity of 50 m/s. At the time of interest, the angle to the target is $\alpha T = -30^\circ$. The range to the target, $r_T = 10$ km.

To simplify the example, we (unrealistically) assume the antenna consists of 16 omnidirectional (isotropic) radiators that are located on the bottom of the aircraft. The array is oriented along the length of the aircraft and the element spacing is $1/2$ wavelength. The radar transmits 16 pulses. Thus, the antenna and waveform are consistent with Example 3. We will use STAP to form a beam and nulls in azimuth-Doppler space. We assume the radar is using an operating frequency of 3 GHz and a PRI of $T = 200 \mu\text{s}$. Since we do not need it, we will leave the pulselength unspecified.

The ring of Figure 16.11 represents the ground region illuminated by the radar at the range to the target (10 km). The radar will also illuminate clutter at ranges of 10 km, plus ranges corresponding to multiples of the PRI. That is, at ranges of $r_T + ncT/2$, where n is an integer and c is the speed of light. For this example, we ignore those clutter returns.

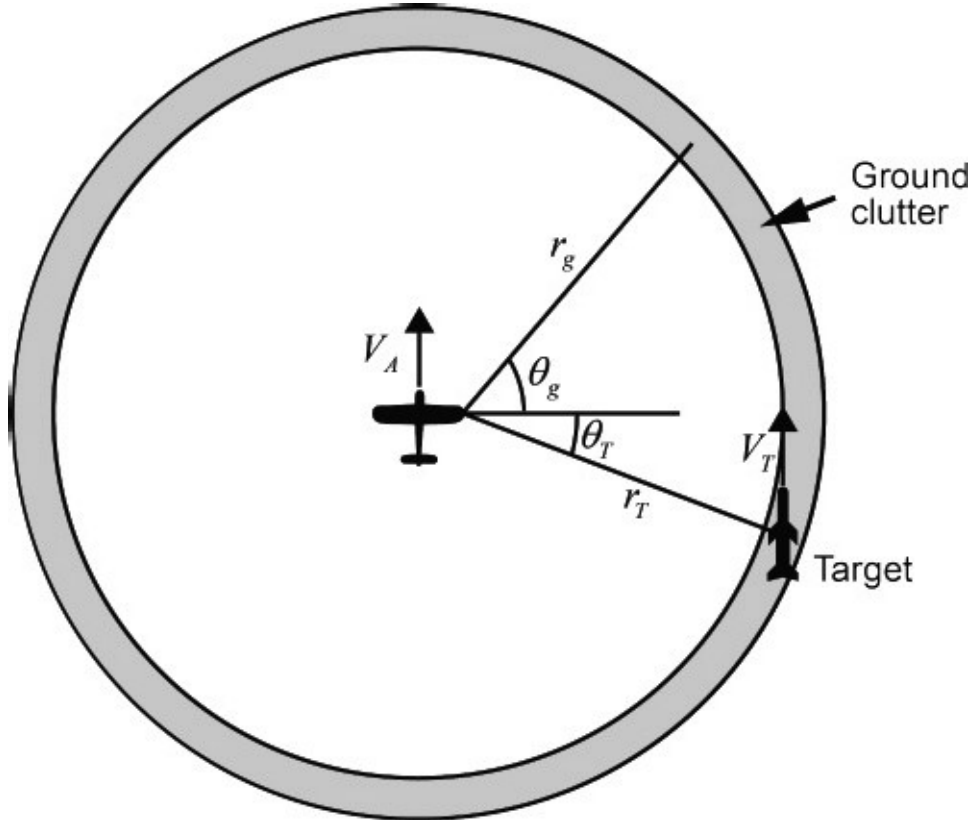


Figure 16.11 Geometry for Example 4.

We assume the per-pulse and per-element SNR and SCR are 0 dB and -50 dB, respectively.

Assuming a normalized noise power of $P_N = 1$ W, the normalized signal power is $P_S = 1$ W, and a normalized interference (clutter) power is $P_I = 10^5$ W. The powers are defined at the output of the single-pulse matched filter.

Given that the aircraft altitude is $h_A = 3$ km and the range to the ground clutter is $r_g = 10$ km, the ground range to the clutter annulus is

$$d_g = \sqrt{r_g^2 - h_g^2} = 9.54 \text{ km} \quad (16.95)$$

We can use this, along with V_T , to compute the Doppler frequency of the ground clutter as

$$f_{dg} = \frac{2V_T d_g}{\lambda r_g} \sin \theta_g = \frac{2V_T d_g}{\lambda r_g} u_g \text{ kHz} \quad (16.96)$$

where we note that u_g varies from -1 to 1 as θ_g varies from 0 to 2π .

Since the aircraft and the target are at the same altitude, we can write the equation for the target Doppler frequency, at the radar, as

$$f_{dT} = \frac{2(V_A - V_T)}{\lambda} \sin(\theta_T) = -0.5 \text{ kHz} \quad (16.97)$$

The target is located at $(\theta_T, f_{dT}) = (-\pi/6, -0.5 \text{ kHz})$ in angle-Doppler space.

Rather than being concentrated at point in angle-Doppler space, the clutter is distributed along a line defined by (16.96). This is illustrated in Figure 16.12, which is a plot like Figure 16.7 with the “beam” in angle-Doppler space steered to (θ_T, f_{dT}) , the target location. The white line is a plot of (16.96) and the black circle indicates the target location. The brightest square is the main beam and the other squares are sidelobes. The vertical axis is $u = \sin(\theta)$ and the horizontal is frequency, f , in kilohertz (kHz). For this example, we assumed the clutter spectrum width was zero. In practice, the width will be not be zero because of internal clutter spectral spread (see Chapter 13) and the aircraft motion. As can be seen, the clutter “line” skirts the main beam and passes close to the target. We did this intentionally to stress the STAP algorithm.

In its basic form, the STAP algorithm developed in this chapter is designed to accommodate only point sources of interference in angle and Doppler. However, we can approximate the continuous line of Figure 16.12 by a series of closely spaced point sources. We choose the point sources so that the spacing between them is much less than the angle and Doppler resolution of the waveform and linear array.

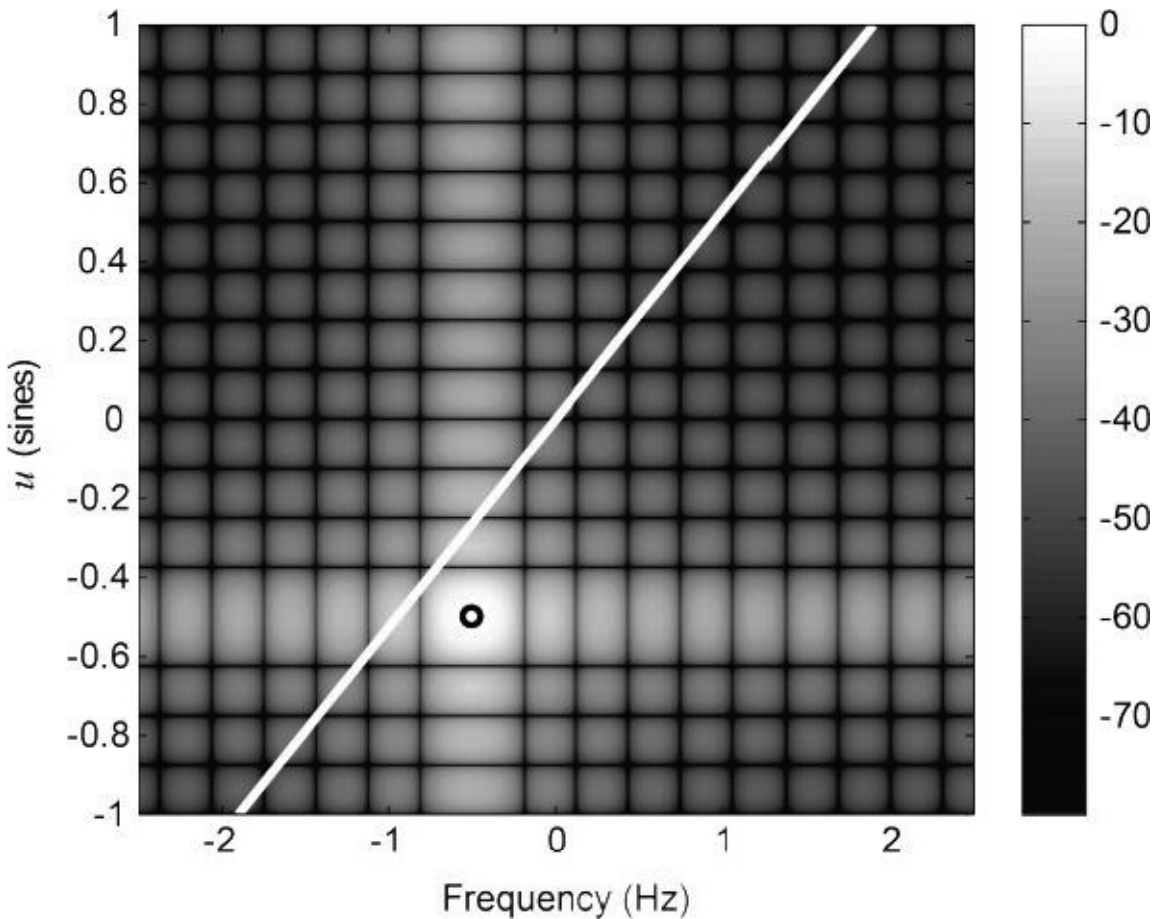


Figure 16.12 Illustration of angle-Doppler plot for interference (white line) and target (black circle), overlaid on the unoptimized angle-Doppler contour plot.

As a reminder, the Doppler resolution of the waveform is equal to the reciprocal of its duration, or $1/16T$ in this case. The angle resolution of the linear array is equal to its length, which is $16(\lambda/2)$ in this case. To satisfy the point source spacing requirement, we represented the line by 40 point sources. We set the angle spacing between the point sources to the length of the line (2 sines) divided by 40. We computed the corresponding f_{dg} from (16.96).

To compute the R matrix, we need to form 40 interference, angle-Doppler steering vectors. The i^{th} angle-Doppler steering vector, $D(i\Delta u, i\Delta f)$, is a $16 \times 16 = 256$ element vector whose elements are given by

$$\exp[j2\pi(ki\Delta f T - ni\Delta u d/\lambda)] \quad n \in [0, 15], \quad k \in [0, 15] \quad (16.98)$$

with $\Delta u = 2/40$ and $\Delta f = 1,900\Delta u$.

With this, we use (16.81) to form the R matrix as

$$R = P_N I + P_I \sum_{i=1}^{40} D(i\Delta u, i\Delta f) D^H(i\Delta u, i\Delta f) \quad (16.99)$$

Finally, we use (16.73), with $\kappa = 1$, to find the optimum weight. We use (16.75), (16.76), and (16.77), with $\theta_s = \theta_T$ and $f_s = f_{dT}$, to find $S(\theta_T, f_{dT})$. The result of computing the weights and

applying them in the STAP processor is shown in Figure 16.13. Note that there is now a deep notch where the white line of Figure 16.12 was located. The SINR before optimization was -31 dB. After optimization, it was 23.5 dB, which is close to the noise limited case of 24.1 dB. This means the STAP processor has effectively attenuated the clutter. As with Figure 16.12, the black circle is the target location and the white square is the main beam.

In this example, we knew location of the target in range, angle, and Doppler and we knew the angle-Doppler distribution of the ground clutter. We also knew the SNR and SCR at the matched filter output for each antenna element and pulse. In practice, we may not know all of this. If the radar was conducting search, we would effectively know the range, angle, and Doppler of interest for each search interrogation. Thus, we would know where we want to steer the angle-Doppler main beam, which means we can compute $S(\theta_T, f_{dT})$. However, we may not know the angle-Doppler distribution or power of the clutter. Without this information, we could not compute R , and would need to determine it from measurements.

As a note, since we assumed a linear array of omnidirectional elements, when the STAP algorithm formed an angle-Doppler beam at $(\theta_T, f_{dT}) = (-\pi/6, -0.5 \text{ kHz})$, it formed another one at $(\theta_T, f_{dT}) = (\pi + \pi/6, -0.5 \text{ kHz})$. We ignored this second beam.

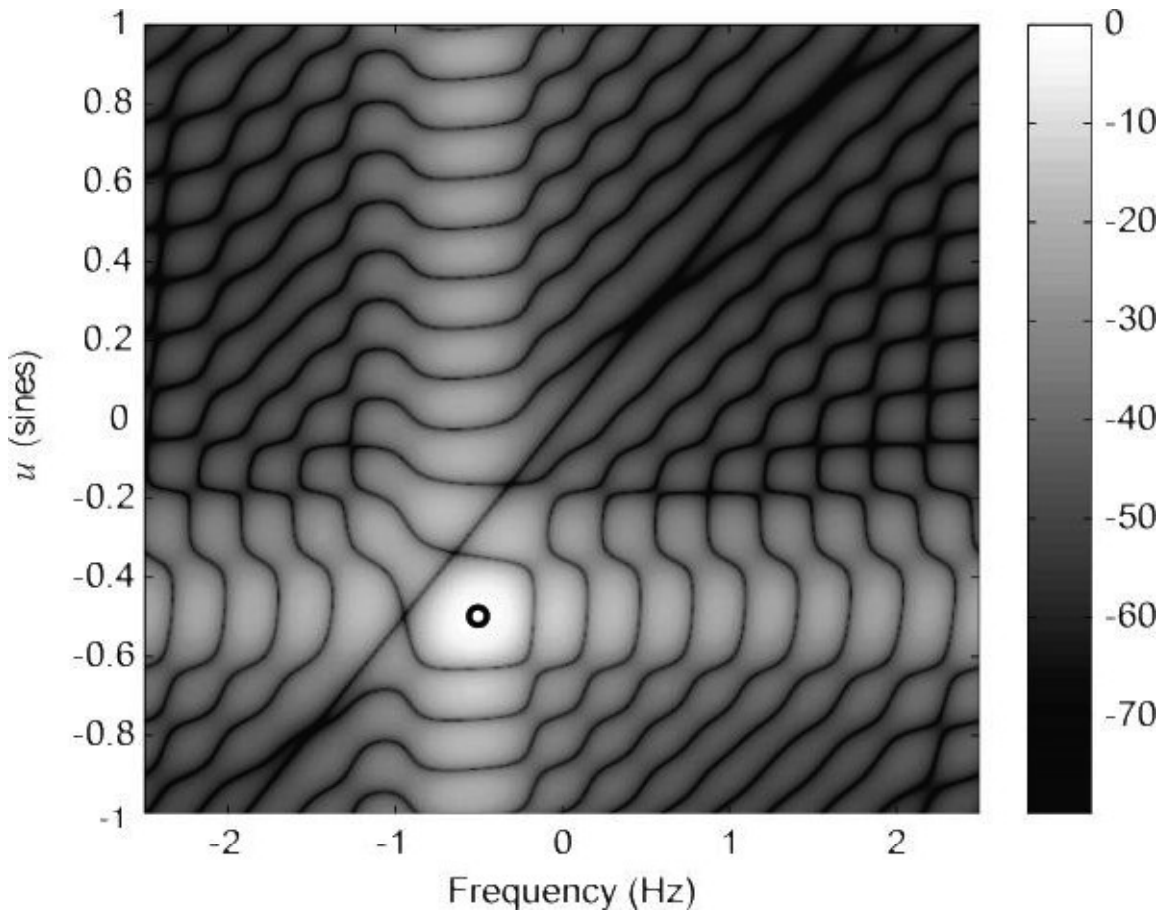


Figure 16.13 Angle-Doppler contour plot with the optimum weights. The black circle is the target location.

16.6 ADAPTIVITY AGAIN

In our work so far, we assumed we knew the various parameters needed to compute the

optimum weights. In particular, we assumed we had enough information to compute the R matrix. In most applications, this is not the case, and we must estimate R through measurements. This is part of the adaptive part of STAP: that the environment is probed and the results are used to experimentally formulate the R matrix. A potential procedure for doing this follows.

For each antenna element (T/R module) and pulse, we sample the combined noise and interference in range cells we believe contain the interference but not the target.⁶ We then use the samples to estimate R . Specifically, if we write the combined noise and interference voltage on a particular sample as V_{N+I}^l , we can form an estimate of R as

$$\hat{R} = \frac{1}{L} \sum_{l=1}^L V_{N+I}^l \left(V_{N+I}^l \right)^H \quad (16.90)$$

where L is the number of samples taken. As a point of clarification, it should be noted that V_{N+I}^l is a KN element vector.

A question that arises is: how large does L need to be? If $L = 1$, we will be multiplying a KN element vector by its Hermitian to produce an KN by KN matrix. This matrix will have a rank of 1 since it was formed as the outer product of two vectors and thus has only one independent column. This means that \hat{R} has only one nonzero eigenvalue, is thus singular, and \hat{R}^{-1} does not exist. Because of this, solving for w by the previous method will not work.

Given V_{N+I}^l consists of random variables, there is a chance that \hat{R} will have a rank equal to L (for $L \leq KN$). Thus, to have any chance of obtaining a \hat{R} that is nonsingular, at least KN samples of V_{N+I}^l must be taken. As L becomes larger, R will converge to reasonable approximation of R , and will be nonsingular. A relation that gives an idea of how large L must be is [11]

$$\rho = \frac{L - MN + 2}{L + 1} \quad L \geq MN \quad (16.91)$$

In this equation, ρ is the ratio of achievable SINR with \hat{R} to the SINR improvement when the actual R is used. For $L = KN$

$$\rho = \frac{MN - MN + 2}{MN + 1} = \frac{2}{MN + 1} \quad (16.92)$$

which says that the SINR improvement actually achieved will be significantly less than the theoretical SINR improvement possible with the actual R . As a specific example, in Examples 3 and 4, $KN = 256$. Thus, the expected SINR based on 256 samples of V_{N+I}^l will be 2/257 or about 21 dB below the optimum SINR improvement. If we increase L to $2KN$ or 512 samples we would get

$$\rho = \frac{2MN - MN + 2}{2MN + 1} \approx \frac{1}{2} \quad (16.93)$$

Thus, the expected SINR improvement based on $\hat{\mathbf{R}}$ would be about 3 dB below the optimum SINR improvement. However, we note that this represents a large number of samples, which will require extensive time and radar resources. Also, for the aircraft case of Example 4, the environment would change before the STAP algorithm could gather enough samples to form the $\hat{\mathbf{R}}$ matrix. We will briefly address this in the next section.

16.7 PRACTICAL CONSIDERATIONS

In practice, it may be possible to use fewer samples of \mathbf{V}_{N+I} if we have a reasonable estimate of the receiver noise power. We would use the aforementioned approximation to form an estimate of \mathbf{R}_I , the interference covariance matrix. If we term this estimate $\hat{\mathbf{R}}_I$, we would form $\hat{\mathbf{R}}$ from

$$\hat{\mathbf{R}} = \hat{\mathbf{R}}_I + P_N I \quad (16.94)$$

where P_N is the receiver noise power estimate (per antenna element and pulse). This approach is termed *diagonal loading* [11, 22, 23]. Adding the term $P_N I$ ensures that $\hat{\mathbf{R}}$ will be positive definite and that $\hat{\mathbf{R}}^{-1}$ exists.

With this method, the number of samples, L , can theoretically be as small as the anticipated number of interference sources [11]. Note that this will generally be much smaller than KN .

This method can have problems in that sometimes $\hat{\mathbf{R}}$ can become ill-conditioned [14], which can cause the optimization to put nulls in the wrong locations. To circumvent this problem, it may be necessary to use more samples in the computation of $\hat{\mathbf{R}}_I$ and/or artificially increase P_N . Taking more samples is problematic because this requires an extra expenditure of time and radar resources. However, increasing P_N will cause the SINR improvement to degrade, potentially to unacceptable levels.

For the aircraft clutter problem, it may be possible to use aircraft information such as altitude or velocity to form somewhat of an analytical estimate of the clutter distribution over angle-Doppler space. Still another approach suggested in [24] is somewhat of an extension of the method used in sidelobe cancellation. Specifically, a portion of the array would be used to gather data and another portion would be used in the actual STAP algorithm. This would reduce the degrees of freedom available to the STAP algorithm, but it may make it possible to afford clutter rejection that could be obtained by other means.

More information about these and other practical aspects of STAP can be found in [3, 11–13, 24].

16.8 EXERCISES

1. Show that (16.1) follows from (16.4).
2. Derive the form of (16.11). Specifically, show that R_n is a diagonal matrix.
3. Derive (16.17).
4. Derive (16.24). Specifically, explain why the double sum reduces to a single sum.
5. Derive (16.28) starting with (16.27).
6. Implement a spatial optimization algorithm and generate the plot of Example 1.
7. Repeat Exercise 6 with interference 1 located at 4° instead of 18° . This places the interference slightly more than $\frac{1}{2}$ beamwidth from the target. You will note that the algorithm places a null in the main beam and moves the peak of the mainbeam slightly off of the target.
8. Derive (16.38) using (16.36) and (16.37).
9. Implement a temporal optimization algorithm and generate the plot of Example 2.
10. Implement a space-time optimization algorithm and generate the four plots of Example 3.
11. Repeat Exercise 10 with the second target located at $(\theta_{s2}, f_{d2}) = (34^\circ, -217 \text{ Hz})$. Note the difference in the angle-Doppler maps when compared to Figures 16.9 and 16.10.

References

- [1] Melvin, W. L., "A STAP Overview," *IEEE Aerosp. Electron. Syst. Mag.*, vol. 19, no. 1, Jan. 2004, pp. 19–35.
- [2] Brennan, L. E., and I. S. Reed, "Theory of Adaptive Radar," *IEEE Trans. Aerosp. Electron. Syst.*, vol. 9, no. 2, Mar. 1973, pp. 237–252.
- [3] Klemm, R., ed., *Applications of Space-Time Adaptive Processing*, London, UK: Institute of Engineering and Technology, 2004.
- [4] Sjogren, T. K. et al., "Suppression of Clutter in Multichannel SAR GMTI," *IEEE Trans. Geosci. Remote Sens.*, vol. 52, no. 7, Jul. 2014, pp. 4005–4013.
- [5] Wei, L. et al., "Application of Improved Space-Time Adaptive Processing in Sonar," *2012 Int. Conf. Comput. Sci. Electron. Eng. (ICCSEE)*, vol. 3, Hangzhou, China, Mar. 23–25, 2012, pp. 344–348.
- [6] Ahmadi, M., and K. Mohamed-pour, "Space-Time Adaptive Processing for Phased-Multiple-Input–Multiple-Output Radar in the Non-Homogeneous Clutter Environment," *IET Radar, Sonar & Navigation*, vol. 8, no. 6, Jul. 2014, pp. 585–596.
- [7] Dan, W., H. Hang, and Q. Xin, "Space-Time Adaptive Processing Method at Subarray Level for Broadband Jammer Suppression," *2011 IEEE Int. Conf. Microwave Tech. & Comput. Electromagnetics (ICMTCE)*, Beijing, China, May 22–25, 2011, pp. 281–284.
- [8] Zei, D., et al., "Real Time MTI STAP First Results from SOSTAR-X Flight Trials," *2008 IEEE Radar Conf.*, Rome, Italy, May 26–30, 2008, pp. 1–6.
- [9] Paine, A. S. et al., "Real-Time STAP Hardware Demonstrator for Airborne Radar Applications," *2008 IEEE Radar Conf.*, Rome, Italy, May 26–30, 2008, pp. 1–5.
- [10] Nohara, T. J. et al., "SAR-GMTI Processing with Canada's Radarsat 2 Satellite," *IEEE 2000 Adaptive Syst. Signal Proc., Commun., Control Symp.*, Lake Louise, Alberta, Canada, Oct. 1–4, 2000, pp. 379–384.
- [11] Guerci, J. R., *Space-Time Adaptive Processing for Radar*, 2nd ed., Norwood, MA: Artech House, 2014.
- [12] Klemm, R., *Principles of Space-Time Adaptive Processing*, 3rd ed., London, UK: Institute of Engineering and Technology, 2006.

- [13] Klemm, R., *Space-Time Adaptive Processing: Principles and Applications*, London, UK: Institute of Engineering and Technology, 1998.
 - [14] Franklin, J. N., *Matrix Theory*, Englewood Cliffs, NJ: Prentice-Hall, 1968.
 - [15] Urkowitz, H., *Signal Theory and Random Processes*, Dedham, MA: Artech House, 1983.
 - [16] Shores, T. S., *Applied Linear Algebra and Matrix Analysis*, New York: Springer, 2007.
 - [17] Widrow, B., et al., "Adaptive Antenna Systems," *Proc. IEEE*, vol. 55, no. 12, Dec. 1967, pp. 2143– 2159.
 - [18] Nitzberg, R., *Adaptive Signal Processing for Radar*, Norwood, MA: Artech House, 1992.
 - [19] Nitzberg, R., *Radar Signal Processing and Adaptive Systems*, Norwood, MA: Artech House, 1999.
 - [20] Manolakis, D. G., et al., *Statistical and Adaptive Signal Processing: Spectral Estimation, Signal Modeling, Adaptive Filtering, and Array Processing*, Norwood, MA: Artech House, 2005.
 - [21] Golan, J. S., *The Linear Algebra A Beginning Graduate Student Ought to Know*, 2nd ed., New York: Springer, 2012.
 - [22] Gabriel, W. R., "Using Spectral Estimation Techniques in Adaptive Processing Antenna Systems," *IEEE Trans. Antennas Propag.*, vol. 34, no. 3, Mar. 1986, pp. 291–300.
 - [23] Carlson, B. D., "Covariance Matrix Estimation Errors and Diagonal Loading in Adaptive Arrays," *IEEE Trans. Aerosp. Electron. Syst.*, vol. 24, no. 4, Jul. 1988, pp. 397–401.
 - [24] Wirth, W. D., *Radar Techniques Using Array Antennas*, London, UK: IEE Press, 2001.
-

¹ We will restrict the development to linear arrays as a convenience. The extension to a planar array is reasonably straightforward.

² Consistent with other developments in this book, we are using complex signal notation as a convenient means of representing the amplitude and phase of RF or IF signals.

³ In Chapter 12, we used W instead of W^H . We made the switch here to be more consistent with the notation used in STAP.

⁴ As a caution $R(\theta)$ is the radiation pattern, which is not to be confused with the covariance matrix, R [without (θ)].

⁵This carries the assumption that the radar is operating unambiguously in range.

⁶ In practice, we can allow the range cells to contain the target return if the overall SNR and SIR (signal-to-interference ratio) is very small for each antenna element and pulse.